

COMPARING ANALYTICAL AND NUMERICAL CALCULATIONS OF SHIELDING EFFECTIVENESS OF PLANAR METALLIC MESHES WITH MEASUREMENTS IN CASCADED REVERBERATION CHAMBERS

D. Månsson* and A. Ellgardt

Division of Electromagnetic Engineering, Royal Institute of Technology (KTH), Teknikringen 33, Stockholm 100 44, Sweden

Abstract—Large electrical systems or facilities can be satisfactorily shielded by using low-cost meshed metallic nets. Here the shielding effectiveness for two such planar meshes is calculated analytically and verified both experimentally by using cascaded reverberation chambers as well as numerically with results computed using a full wave electromagnetic solver. It is shown that all three methods agree and, in addition, that non-square shaped aperture meshes can be handled with an equivalent square area shaped aperture.

1. INTRODUCTION

The increased use of sophisticated electrical and electronic systems to control and monitor critical infrastructure components is a potential EMC problem. With the concept of electromagnetic topology in mind [1], many of the systems that require electromagnetic shielding are physically very large with many apertures and cables entering the facility that needs to be handled correctly. The cause of the electromagnetic interference (EMI) can, e.g., be lightning strikes (that cause both surge currents and radiated fields) or radio and radar stations (where incidents due to fields of high power have been recorded, see [2] or [3] for an overview). Another concern that justifies the use of protection from EMI is the threat of intentional EMI (IEMI) [3]. IEMI is the intentional malicious use of electromagnetic energy to cause upsets in, or damage to, electronic systems [4] and is today also considered a large hazard to critical infrastructure and its subsystems.

Received 15 June 2012, Accepted 16 July 2012, Scheduled 17 July 2012

* Corresponding author: Daniel Månsson (daniel.mansson@ee.kth.se).

Using filters and surge protective devices to mitigate EMI becomes, due to the large cost, in many cases not an option for protecting large distributed systems. An alternative solution is to shield the enclosure holding the equipment with commercial EMC shields. However, such are often deemed too expensive and thus critical equipment are often unprotected due to short term financial gains. A low-cost, but still satisfactorily effective shielding method is needed. One such type of “good enough shield” is the low-cost meshed metal net (approximately $0.5\text{€}/\text{m}^2$ according to wholesaler). Using such low cost, easily installable meshes is a mitigation method that could convince system owners to take at least some action, as opposed of today where none are taken at all. By default, in this paper only radiated EMI is considered.

The simplest case of a metal mesh is the polarizer which is constructed solely by metal wires that are parallel to each other with equidistant spacing in a plane. How much and in which direction an incident electromagnetic wave is scattered depends on, besides the angle of incidence, the spacing between the wires and the thickness of the wires. For this case, an electromagnetic wave with polarization that is parallel to the wires will be scattered by the mesh and a wave orthogonal to the wires will pass through the mesh. To increase the shielding for this polarization we can add additional wires that are not parallel to the other set of wires. The best choice is of course to put them orthogonal to the first set.

Most common metal meshes are relatively effective up to a few GHz (actual adequacy depending on the specific mesh dimensions) as well as easily installable in both fixed installations and for shielding of equipment. The idea of using metallic meshes as shields is not new and it is well known that these acts as Faradays cages if the aperture dimensions are electrically small, but calculating the exact shielding effectiveness accurately isn't trivial. However, approximate analytical approaches have been suggested (e.g., [5]) and in this paper we confirm that the value for the shielding effectiveness that is derived through one such relatively simple analytical approach agrees well with values obtained both through experiments and/or numerical simulations for two different types of meshes over a wide frequency band.

In the work presented here two types of normal commercial meshes were studied; one mesh with relatively large hexagonal apertures (with wire radius $\approx 0.3\text{ mm}$, see Figure 1) and one mesh with smaller square apertures (with side lengths $\approx 4\text{ mm}$ and wire radius $\approx 0.45\text{ mm}$).

The structure of this paper is as follows; first the analytical approach is discussed, followed by an explanation of the experiments performed and then the numerical simulations are discussed. After

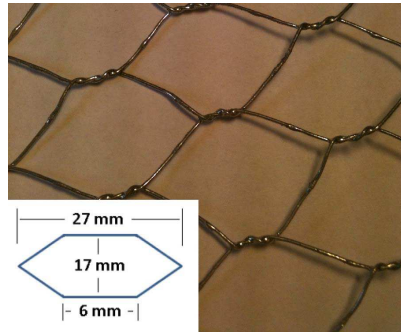


Figure 1. The mesh with hexagonal apertures.

this, the three methods are compared followed by discussions and conclusions.

2. ANALYTICAL APPROACH

The shielding effectiveness of a planar wire meshed screen with bonded junctions can, when the mesh dimensions are small compared to the wavelength, be described through the equivalent sheet impedance [5] of the mesh. The polarization-independent shielding effectiveness (1a) and the associated power transmission coefficient (1b) of a mesh with a square aperture of length “*a*” and wire radius “*r*” can then be described with (see [5] for details):

$$SE(\omega, \theta) = -10 \log_{10} \left\{ \frac{1}{2} |T_1(\omega, \theta)|^2 + \frac{1}{2} |T_2(\omega, \theta)|^2 \right\} \quad (1a)$$

$$T_{tot}(\omega, \theta) = -SE(\omega, \theta). \quad (1b)$$

$T_1(\omega, \theta)$ and $T_2(\omega, \theta)$ are the transmission coefficients (for different frequencies and angles of incidence) for the polarization of TE and TM modes, respectively and given by:

$$T_1(\omega, \theta) = \frac{(2Z_{s1}(\omega)/Z_0) \cos \theta}{1 + (2Z_{s1}(\omega)/Z_0) \cos \theta}, \quad (2a)$$

$$T_2(\omega, \theta) = \frac{(2Z_{s2}(\omega)/Z_0)}{(2Z_{s2}(\omega)/Z_0) + \cos \theta}. \quad (2b)$$

The angle of incidence θ is measured from the normal of the planar sheet. Besides the free-space impedance, Z_0 , the comprising parts of

(2a) and (2b) are:

$$Z_{s1}(\omega) = Z_w a + j\omega L_s, \quad (3)$$

$$Z_{s2}(\omega) = Z_{s1} - \frac{j\omega L_s}{2} \sin^2 \theta, \quad (4)$$

where Z_{S1} and Z_{S2} are the eigenvalues of the sheet impedance operator, corresponding to the TE and TM mode, respectively. Also, the sheet inductance L_S and the wire impedance per unit length Z_W (approximated to its DC resistance) are given by:

$$L_s = \frac{\mu_0 a}{2\pi} \ln \left\{ \left(1 - e^{-2\pi r/a} \right)^{-1} \right\}, \quad (5)$$

$$Z_w = (\pi r^2 \sigma)^{-1}. \quad (6)$$

The approximation of using the DC wire resistance instead of the wire impedance is motivated by the fact that no discernible effect was seen in (1b), for the frequencies and structures investigated here, when adding the skin effect to (6). Thus, it becomes straightforward, for a given mesh (with square apertures), to calculate the shielding effectiveness for different situations (θ and ω).

It is important to note that if the apertures of the mesh are not square (e.g., hexagonal) as required by the approach above, an equivalent square area can be calculated. The justification for this (see Figures 99 and 100 in [6]) is that the polarizability of an aperture is not very sensitive to the actual shape of the aperture and depends almost entirely upon the width-to-length ratio. Thus, a mesh with hexagonal apertures can be translated to a mesh with square apertures with equivalent areas to the hexagons (see Figure 2). Thus, in the mesh with hexagonal apertures, these had, individually, such an area that they corresponded to a square aperture with side length ≈ 17 mm. Note that in [6] (and the sources it refers to) frequency limitations for doing this is not discussed but the good correspondence between

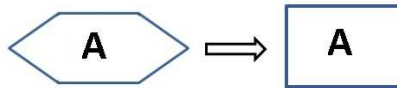


Figure 2. A hexagonal aperture of area A can be translated to a square shaped aperture also with area A and, thus, side length \sqrt{A} . Thus, this concept of equivalent square area can be employed on the mesh with hexagonal apertures to translate it to a mesh with square apertures to be able to use (1a).

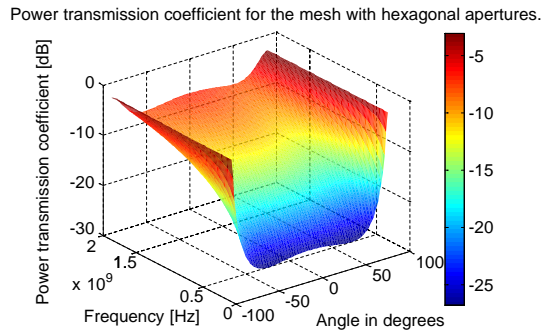


Figure 3. Using the method of an equivalent square area and (1b) the power transmission coefficient, as a function of frequency and angle of incidence, can be calculated for the mesh with hexagonal apertures.

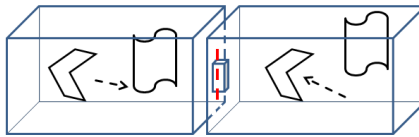


Figure 4. The cascaded reverberation chambers with the bridge, where the mesh is installed, shown.

the different methods used here to calculate the power transmission coefficient (see Figure 5) and the frequency span generally discussed in [6] is an indicator that this is not a critical concern here. However it should be noted, as Figure 101 of [6] clearly shows, that a cross shaped aperture have to, for some cases, be handled with care.

Using (1a) the polarization independent shielding effectiveness for the mesh with hexagons can then be calculated. As can be seen in Figure 3 the power transmission coefficient of the mesh is significantly higher (lower shielding) for fields with large incidence angles than fields with incidence normal to the surface and that higher frequencies leads to higher power transmission.

3. EXPERIMENTAL RESULTS

For the experimental verification of the shielding effectiveness of the meshes, cascaded reverberation chambers were used (see Figure 4) (sometimes the term “nested” is used also for this configuration, see [7] for more details on the chambers). Also it is assumed that the

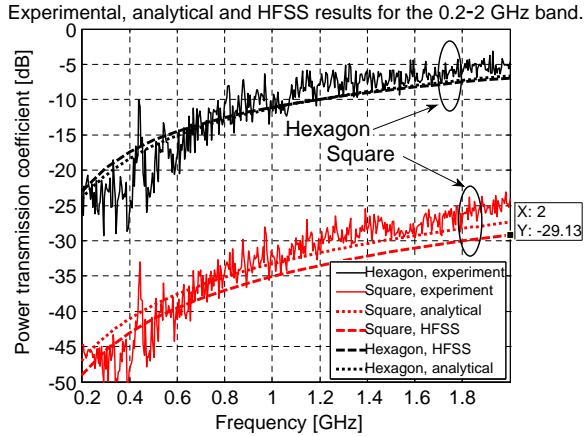


Figure 5. Comparison, in the 0.2–2 GHz band, between experimental data, analytical approach, and numerical simulations done with HFSS. The two cases are shown, mesh with small square apertures and mesh with large hexagonal apertures. As discussed in the text, the sharp peak around 400 MHz is deemed to be from leakage around the frame.

average over all angles of incidence (from the analytical approach) is an accurate description of the randomization of angles of incidence in the reverberation chamber. This assumption stands on good theoretical and experimental ground, as much solid theoretical work assuming this (see, e.g., [8] or [9]) is validated by numerous experimental results. Averaging over the angles of incidence is used below to compare the different datasets obtained here (see Figures 5, 6 and 7).

The two chambers are connected via a short bridge having a square cross-section (approximate side length of 0.3 m) and a length of approximately 0.2 m. The size of the transmitting chamber is approximately 5.1 * 3.0 * 2.5 m and the receiving chamber 3.6 * 2.5 * 3.1 m. First, the transmission loss from one chamber to the other was measured without any mesh installed at the interconnecting bridge. This acts as a baseline and is used to normalize the shielding effectiveness of the meshes to remove the effects on the attenuation due to this interconnecting bridge. Thus, we can safely argue that the shielding effectiveness measured is predominately a result of the meshes themselves (with the exceptions discussed below and in Section 6.1). The two paddles in the two chambers are used in mode stepping (tuning), where, for each position of the paddle in the transmitting chamber, several positions of the paddle in the receiving chamber were used. All in all, 20 * 20 positions of the paddles were used which gives

Experimental and analytical results for the 2-18 GHz band.

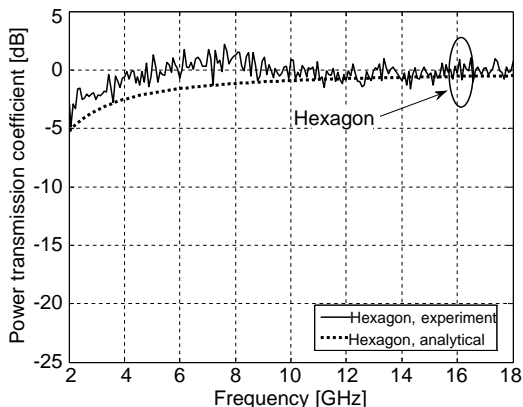


Figure 6. Comparison, in the 2–18 GHz band, between experimental data and the analytical approach, for the mesh with large hexagonal apertures. As discussed in the text, the numerical simulations are not performed for this case.

Experimental, analytical and HFSS results for the 2-18 GHz band.

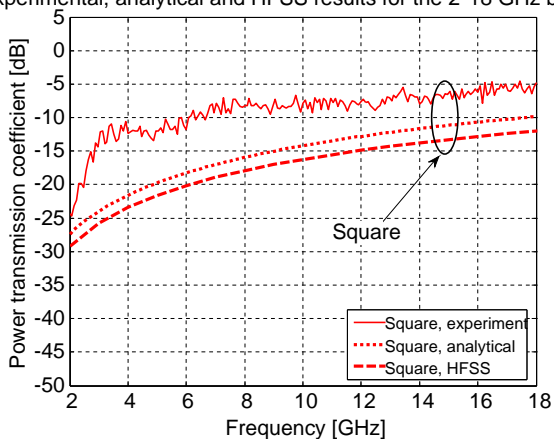


Figure 7. Comparison, in the 2–18 GHz band, between experimental data, analytical approach, and numerical simulations done with HFSS for mesh with square apertures. The difference between the experimental data and the two other datasets (for this case) is believed to be due to the Q value being too low, in the reference case, for useful comparison.

400 independent samples for each frequency used. Keeping the low frequency limit of the chambers in mind, this is enough to acquire the required random and isotropic properties of the reverberation chambers [7]. The obtained shielding effectiveness, after normalization (as described above), is shown in Figures 5, 6 and 7 for the two meshes and frequency bands studied.

The likely explanation for the sharp peak in the power transmission coefficient around 400 MHz (see Figure 5) is that it corresponds to the leakage around the 29×29 cm frame in the interconnecting bridge to which the meshes are installed. A resonance is expected around a frequency equal to approximately 60% of the circumference of the slot, i.e., around 0.43 GHz [10], which fits very well what is seen.

4. NUMERICAL SIMULATIONS

Shielding effectiveness can be studied numerically using, e.g., methods of moments (MOM), finite element method (FEM) or finite difference time domain (FDTD) approaches to compute the transmission through meshes. These methods are in general restricted by memory requirements to structures of a few wavelengths or infinite periodic structures where a unit cell (i.e., aperture) with periodic boundaries can represent the structure. A very convenient way to analyze the shielding properties of a type of wall (e.g., a mesh) is to assume that it is infinite in extent. This reduces the problem to a unit cell with periodic boundary conditions for a periodic structure. For an infinite periodic structure the spectra is discrete and a plane wave will be transmitted and reflected in discrete directions. These waves are the solutions to the wave-equation for periodic domain, and are called Floquet-modes.

When the unit cell side is half a wavelength of the incident plane wave, there is only one Floquet-mode each for the TE- and TM-component of the transmitted field which is in a single direction. When the frequency is increased the spacing between the wires eventually becomes equivalent to one wavelength and additional Floquet-modes start to propagate in different directions. Thus, for higher frequencies the incoming plane wave will be transmitted in multiple directions that will change with frequency.

The transmission through the two meshes was here numerically investigated by using HFSS (High Frequency Structural Simulator) [11]. HFSS is a commercial software package using the finite elemental method to solve the electromagnetic interaction with metallic structures problems and it is often used in antenna and microwave filter calculations. The numerical computations were used here to verify

that the simple analytical results and the experimental results are viable, and to solidify the conclusions drawn from these.

The meshed screen is modeled as an infinite frequency selective surface. The regular mesh is a dual periodic structure which is made of small identical connected wire segments. If the incident wave is a plane wave the infinite structure can be exactly represented by a single unit cell with quasi periodic boundary conditions [12,13] for boundaries with a normal in the sheet plane. The fields on two opposing boundaries are identical except for a phase shift that depends on the incidence angle of the planar wave. Please note that, due this approach of using periodic structures it is not possible to directly implement the hexagonal shape. Thus, the approach of using an equivalent square area is also used in the numerical simulations of the hexagonal mesh. The shielding effectiveness is then computed using Equation (1a) and averaging over the angles of incidence as described below by (7). As the results for all of the three methods converge in the case of the mesh with hexagons, numerical simulations were not performed to save time.

5. COMPARISON

The analytical approach (and the numerical simulations) gives a shielding effectiveness that is dependent on both the angle of incidence and frequency (besides the dimensions of the apertures) and needs to be modified before comparison with the experimental data. In the reverberation chamber, for one complete revolution of the paddle in the transmitting chamber, the angle of incidence of the fields towards the installed mesh is randomized (with, ideally, equal likelihood for every angle). Thus, to compare the datasets the arithmetic mean of the inner sum in (1a) is computed (over the angles of incidence in the interval $(-\pi/2 : \pi/2)$) before the logarithm is taken, i.e.,

$$SE_{aver} = -10 \log_{10} \left\{ \frac{1}{n} \sum_{i=1}^n \left(\frac{1}{2} |T_1(\omega, \theta_i)|^2 + \frac{1}{2} |T_2(\omega, \theta_i)|^2 \right) \right\}. \quad (7)$$

That is, the average of the angle of incidence, for each frequency, is taken and the result is shown, in comparison to the experimental data, in Figures 5, 6 and 7. For the results produced by the numerical simulations the procedure is the same. The reason for doing this averaging over the angles of incidence is that it is then possible to compare with experimental results from reverberation chambers but also that in general the propagation direction, of the fields causing the electromagnetic interference, is unknown.

As can be seen the experimental data, analytical approach and numerical simulations agree very well, for both meshes studied, in the 0.2–2 GHz band (see Figure 5). For the mesh with hexagon apertures and the 2–18 GHz frequency band the numerical result still coincides well with the analytical results but not with the experimental results (see Figure 7). This is in part deemed to be a measurement artifact and is discussed in Section 6.1.

In addition, some of the seen discrepancies between the three approaches are also deemed to be from measurement error when measuring the relatively small dimensions of the apertures.

6. DISCUSSION

6.1. On Observed Measurement Artifact

The difference above 2 GHz (see Figure 7), for the mesh with square apertures, between measured, analytical and simulated results can, at least partly, be explained by the fact that the Q -values in both chambers are lower in the reference case (i.e., the case with open interconnecting bridge and no mesh installed) compared to the case where the mesh is installed. This means that the field strengths in both chambers are too low in the reference case. In the chamber with the transmitting antenna this could theoretically be compensated for by increasing the input power in order to get the same power density irradiating the aperture as when the mesh is installed and irradiated. In the chamber with the receiving antenna a correction could be made to the power picked up by the receiving antenna in proportion to the change in Q -value, thereby keeping the relation between the power picked up by the receiving antenna and the power transmitted into the chamber constant. This procedure is used in [14]. Since neither of these measures was made in the present case the power picked up by the receiving antenna was hence too low in the reference case. All this means that we expect the measured attenuation to be lower than expected from theory. As can be seen in Figure 7, this is also the case for the mesh with square apertures in the 2–18 GHz frequency band. For the mesh with large hexagonal large apertures the effect is expected to be much smaller due to its lower attenuation, i.e., its attenuation is similar to that of the reference case, i.e., the open aperture. This effect due to the reduced value of Q -value in the reference case was recently also reported in [15].

Unfortunately it was not possible for to redo the measurement campaign and the reason why we still chose to include this data here (Figure 7) is that it still shows the good agreement between the analytical approach and the numerical simulation but also that

it highlights an interesting and important measurement phenomenon that needs to be understood when performing measurements in reverberation chambers.

6.2. On Shielding with Meshes in General

For electrically small apertures the transmitted fields decline rapidly and are significantly lower even at very short distances (compared to the wavelength of the incident field) after the mesh [6]. Thus, in our case, the wire meshes studied here could be considered suitable as shields (approximately 20 dB shielding) for frequencies up till, in the order of, a few hundreds of megahertz and a few gigahertz, respectively.

A vulnerable part of most fixed installations, are the many and long cables connected between control equipment and power equipment. Such cables are often running in unshielded cables trenches. Electromagnetic fields could easily couple to them and the induced common mode current interfere with connected equipment. For the frequencies studied here, these low cost shields could be used to a great extent to shield these cable by constructing a shielded structure in the trench and around the cables. As with all shielding situations it is important that the object to be protected is not placed too close to apertures, here the mesh boundary (as discussed above). In addition, other structures, such as buildings containing backup power or redundant systems, could also be easily and cost effectively shielded. (Note that normal shielding installation practices still applies, e.g., seams and connections in the shielding boundaries have to be handled correctly as well as making sure that individual wires in the meshes have a good electrical contact between each other). For such cases, it is of great benefit to investigate the actual placement of the equipment inside the facility to decrease the chance of exposure to electromagnetic fields exceeding the threshold levels for different forms of upsets.

It is important to remember when designing a shielded system, based on a wire mesh screen that the attenuation is, as shown in Figure 3, highly dependent on the angle of incidence of the field. Thus, for a given situation this must be taken into account when estimating a safety distance between the equipment inside and the shield for a given attenuation factor. However, over a large timespan the angles of incidence for the EMI should be considered to be fairly random and, thus, the curves presented here (see Figures 5, 6 and 7) gives the transmission through the mesh for the values that could be expected, on average, for many random disturbances.

Also it is worth noting that the analytical approach in [5] using equivalent sheet impedance to calculate the shielding effectiveness

seems to work well even though the mesh dimensions are in the order of the wavelength.

Finally, it is important to remember that a well shielded enclosure can act as a reverberation chamber due to the Q -value that is created. Thus, fields that penetrate the shield could get amplified and equipment inside the enclosure would get subjected to fields higher than might otherwise not be present if the shield was not installed.

7. CONCLUSION

In this paper, it is shown that simple analytical approaches to determining shielding effectiveness coincide well, for the studied mesh types and frequency bands, with experimentally obtained data and/or numerical simulations. In addition, it is specifically seen that:

- 1 Meshes with apertures of non-square shape can be handled very well with an equivalent square area (as the polarizability of the aperture is almost independent of the actual shape the aperture).
- 2 Averaging (arithmetic mean) over all angles of incidence is here a good description of the randomization in the cascaded reverberation chambers, which can be used to compare different methods of deducing the shielding effectiveness for different samples and materials.
- 3 If calculations to deduce the shielding effectiveness are made such low cost non-exceptional commercial meshes are viable solutions for creating a large shielded enclosure or to shield cable trenches.

ACKNOWLEDGMENT

Olof Lundén, formerly at the Swedish Defence Research Agency (FOI), is greatly thanked for his invaluable help in acquiring the experimental data. Mats Bäckström, at SAAB Aeronautics, is also greatly thanked.

REFERENCES

1. Vance, E. F., "Shielding and grounding topology for interference control," *Interaction Notes*, C. E. Baum (Ed.), Air Force Weapons Laboratory, Note 306, Apr. 1977.
2. IEC Standard, 61000-1-5, "Electromagnetic compatibility (EMC) — Part 1-5: General — High power electromagnetic (HPEM) effects on civil systems," 2004.

3. Radasky, W., C. E. Baum, and M. W. Wik, "Introduction to the special issue on high-power electromagnetics (HPEM) and intentional electromagnetic interference (IEMI)," *IEEE Trans. on Electromagnetic Compatibility*, Vol. 46, No. 3, 314–321, Aug. 2004.
4. URSI the Toronto General assembly, Aug. 13–21, 1999, Accessible via <http://ursiweb.intec.ugent.be/Resolutions/99%20Toronto%20Res%20Eng.doc>.
5. Casey, K. F., "Electromagnetic shielding behavior of wire-mesh-screens," *IEEE Trans. on Electromagnetic Compatibility*, Vol. 30, No. 3, Aug. 1988.
6. Lee, K. S. H., *EMP Interaction: Principles, Techniques and Reference Data*, Hemisphere Publishing Corp., Washington, 1986.
7. Bäckström, M. and O. Lundén, "Transmissions cross section of apertures measured by use of nested mode-stirred chambers," FOA-R-96-00359-3.2-SE, Dec. 1996.
8. Hill, D., "Plane wave integral representation for fields in reverberation chambers," *IEEE Trans. on Electromagnetic Compatibility*, Vol. 40, 209–217. Aug. 1998.
9. Bäckström, M., O. Lundén, and P. S. Kildal, "Reverberation chambers for EMC susceptibility and emission," *Review of Radio Science*, 429–451, Wiley-IEEE Press, 2002.
10. Martin, T., M. Bäckström, and J. Lorén, "Transmission cross section of apertures, determined by measurements and FDTD simulations," *Proc. 12th International Zurich, Symposium and Technical Exhibition on Electromagnetic Compatibility*, Feb. 18–20, 1997.
11. www.ansoft.com/products/hf/hfss/, Available 2012-06-14.
12. Amitay, N., V. Galindo, and C. P. Wu, *Theory and Analysis of Phased Array Antennas*, Wiley-Interscience, New York, 1972.
13. Munk, B. A., *Frequency Selective Surfaces: Theory and Design*, John-Wiley, New York, 2000.
14. Holloway, C., D. Hill, J. Ladbury, G. Koepke, and R. Garzia, "Shielding effectiveness measurements of materials using nested reverberation chambers," *IEEE Trans. on Electromagnetic Compatibility*, Vol. 45, No. 2, 350–356, May 2003.
15. Primiani, V. M., F. Moglie, and A. P. Pastore, "Field penetration through a wire mesh screen excited by a reverberation chamber field: FDTD analysis and experiments," *IEEE Trans. on Electromagnetic Compatibility*, Vol. 51, No. 4, 883–891, Nov. 2009.